NASA / TM—1998-207412

The Design of a Transparent Vertical Multizone Furnace: Application to Thermal Field Tuning and Crystal Growth

Walter M.B. Duval
Lewis Research Center, Cleveland, Ohio

Celal Batur and Robert J. Bennett
University of Akron, Akron, Ohio

May 1998

The NASA STI Program Office . . . in Profile

Since its founding, NASA has been dedicated to the advancement of aeronautics and space science. The NASA Scientific and Technical Information (STI) Program Office plays a key part in helping NASA maintain this important role.

The NASA STI Program Office is operated by Langley Research Center, the Lead Center for NASA's scientific and technical information. The NASA STI Program Office provides access to the NASA STI Database, the largest collection of aeronautical and space science STI in the world. The Program Office is also NASA's institutional mechanism for disseminating the results of its research and development activities. These results are published by NASA in the NASA STI Report Series, which includes the following report types:

- TECHNICAL PUBLICATION. Reports of completed research or a major significant phase of research that present the results of NASA programs and include extensive data or theoretical analysis. Includes compilations of significant scientific and technical data and information deemed to be of continuing reference value. NASA's counterpart of peer-reviewed formal professional papers but has less stringent limitations on manuscript length and extent of graphic presentations.

- TECHNICAL MEMORANDUM. Scientific and technical findings that are preliminary or of specialized interest, e.g., quick release reports, working papers, and bibliographies that contain minimal annotation. Does not contain extensive analysis.

- CONTRACTOR REPORT. Scientific and technical findings by NASA-sponsored contractors and grantees.

- CONFERENCE PUBLICATION. Collected papers from scientific and technical conferences, symposia, seminars, or other meetings sponsored or cosponsored by NASA.

- SPECIAL PUBLICATION. Scientific, technical, or historical information from NASA programs, projects, and missions, often concerned with subjects having substantial public interest.

- TECHNICAL TRANSLATION. English-language translations of foreign scientific and technical material pertinent to NASA's mission.

Specialized services that complement the STI Program Office's diverse offerings include creating custom thesauri, building customized data bases, organizing and publishing research results . . . even providing videos.

For more information about the NASA STI Program Office, see the following:

- Access the NASA STI Program Home Page at ***http://www.sti.nasa.gov***

- E-mail your question via the Internet to help@sti.nasa.gov

- Fax your question to the NASA Access Help Desk at (301) 621-0134

- Telephone the NASA Access Help Desk at (301) 621-0390

- Write to:
  NASA Access Help Desk
  NASA Center for AeroSpace Information
  7121 Standard Drive
  Hanover, MD 21076

NASA / TM—1998-207412

The Design of a Transparent Vertical Multizone Furnace: Application to Thermal Field Tuning and Crystal Growth

Walter M.B. Duval
Lewis Research Center, Cleveland, Ohio

Celal Batur and Robert J. Bennett
University of Akron, Akron, Ohio

Prepared for
Technology 2007
sponsored by the NASA Tech Briefs, NASA, The Federal Laboratory Consortium,
and the Technology Utilization Foundation
Boston, Massachusetts, September 22–24, 1997

National Aeronautics and
Space Administration

Lewis Research Center

May 1998

Acknowledgments

We acknowledge the support of the Commercial Technology Office at NASA Lewis Research Center through Gary A.P. Horsham, Comm-Tech Program Manager. Technical discussions with N.B. Singh at Northrop Grumman, S. Trivedi at Brimrose Corporation of America, and M. Kassemi at The National Center for Microgravity Research are gratefully acknowledged. This work was performed in the Microgravity Processing Sciences Branch under a NASA grant, contract number NCC3-367.

Available from

NASA Center for Aerospace Information
7121 Standard Drive
Hanover, MD 21076
Price Code: A03

National Technical Information Service
5287 Port Royal Road
Springfield, VA 22100
Price Code: A03

THE DESIGN OF A TRANSPARENT VERTICAL MULTIZONE FURNACE: APPLICATION TO THERMAL FIELD TUNING AND CRYSTAL GROWTH

Walter M.B. Duval*, Celal Batur†, Robert J. Bennett†

***NASA Lewis Research Center, Cleveland, Ohio 44135**

†University of Akron, Department of Mechanical Engineering, Akron, Ohio 44325–3903

ABSTRACT

We present an innovative design of a vertical transparent multizone furnace which can operate in the temperature range of 25 ^{o}C to 750 ^{o}C and deliver thermal gradients of 2 ^{o}C/cm to 45 ^{o}C/cm for the commercial applications to crystal growth. The operation of the eight zone furnace is based on a self-tuning temperature control system with a DC power supply for optimal thermal stability. We show that the desired thermal profile over the entire length of the furnace consists of a functional combination of the fundamental thermal profiles for each individual zone obtained by setting the set-point temperature for that zone. The self-tuning system accounts for the zone to zone thermal interactions. The control system operates such that the thermal profile is maintained under thermal load, thus boundary conditions on crystal growth ampoules can be predetermined prior to crystal growth. Temperature profiles for the growth of crystals via directional solidification, vapor transport techniques, and multiple gradient applications are shown to be easily implemented. The unique feature of its transparency and ease of programming thermal profiles make the furnace useful in scientific and commercial applications for determining the optimized process parameters for crystal growth.

1.0 INTRODUCTION

One of the fundamental variables in crystal growth applications is the tuning of the thermal gradient, we present an innovative multizone transparent furnace design which allows precise control of the thermal field. The features of the furnace, from the standpoint of technical merit, which make it attractive are its transparency and ease of programming the desired thermal profile. The transparency feature of the furnace lends it the commercial potential for on-line quality control of crystal growth. The scientific application of the furnace is crystal growth of acousto-optic optoelectronic materials such as lead and mercurous halides, nonlinear optics, photonics, low temperature semiconductors and organic crystals, which span the temperature range of 25 ^{o}C to 750 ^{o}C.

For applications to the growth of bulk single crystal growth, it has been widely recognized by many investigators [1-4] that the thermal field affects the crystalline quality. These applications stem primarily from crystals grown by directional solidification for which the macroscopic shape of the solid-liquid interface is used as feedback for quantification of the localized thermal gradient. Though planar interfaces are preferable from the standpoint of minimization of thermal stresses [1], a convex interface may be beneficial for some applications. Thus, there exists benefits for tailoring the thermal profile to achieve certain desired outcomes.

Traditionally, crystals are grown in a two zone Bridgman furnace which provides two temperature baths, a hot and a cold zone, with a thermal gradient between the two zones. Chang and Wilcox [4] showed that the sensitivity of the interface shape can be decreased by inserting a layer of insulation between the cold and hot zone. The insulated layer causes the heat transfer to be unidirectional near the solid-liquid interface; this results in a nearly flat interface. Although this approach is desirable, the insulation layer blocks the view of the solid-liquid interface, which results in the loss of vital information. We introduce the design of a transparent eight zone furnace which allows the tailoring of thermal gradients. Due to its versatility, multiple gradients can be achieved whereby the heat transfer can be made unidirectional over a segment, without the use of insulation, thus preserving the transparency of the furnace. In addition to directional solidification applications, this furnace is useful for crystal growth by the physical vapor transport process which requires a thermal profile with a “hump” used to prevent spontaneous nucleation. This thermal profile has been used by Hartmann and Schonherr [5, 6] to measure crystal growth rates by relaxation. We present the design of the furnace and show thermal profiles of interest for both directional solidification as well as physical vapor transport used in applications to grow crystals.

* Corresponding author, tel. 216-433-5023, fax. 216-433-5033, e-mail: duval@sarah.lerc.nasa.gov

2.0 EXPERIMENTAL DESIGN

2.1 Innovative Furnace Design

The basic characteristic of a crystal growth furnace is a device that allows a uniform thermal gradient to be established inside an enclosure with optimum temperature stability. In addition, this device should allow a range of thermal gradients to be set-up in order to allow optimization of crystal growth parameters, an important feature for directional solidification applications [7, 8]. Through several iterations, Batur et. al. [9,10] , we have constructed an eight zone furnace, shown in Figure 1 (see Appendix for detail), that fulfills our objectives. This furnace consists of two concentric quartz cylinders (high optical grade quartz 'GE-214'), of height 52 cm, inner diameter of 4.3 cm with wall thickness 3mm, and outer diameter of outer cylinder of 6.8 cm with wall thickness of 2 mm . A spiral helical groove, of equal depth and width of 1.27 mm, is imbedded on the outer surface of the inner cylinder with a constant pitch. The heating kanthal wires are imbedded as a continuous coil on the outer surface of the inner cylinder. This allows the heat flux to be nearly uniform azimuthally; in addition the quartz tube act as a low pass filter to damp high frequency noise from the power supply. The outer cylinder which acts as an insulator is split axially, thus consists of two sections which allows for ease of instrumentation. The connection from the furnace, approximately 1.25 to 2 cm from the outer cylinder, to the main power supply requires the joining of the kanthal wire to 99% pure nickel by butt welding. The lower resistance of the nickel minimizes heat loss to the ambient environment. The heating elements (A-1, Kanthal wire) are placed into the spiral ground groove of the inner cylinder in a manner which minimizes the gap between heating elements.

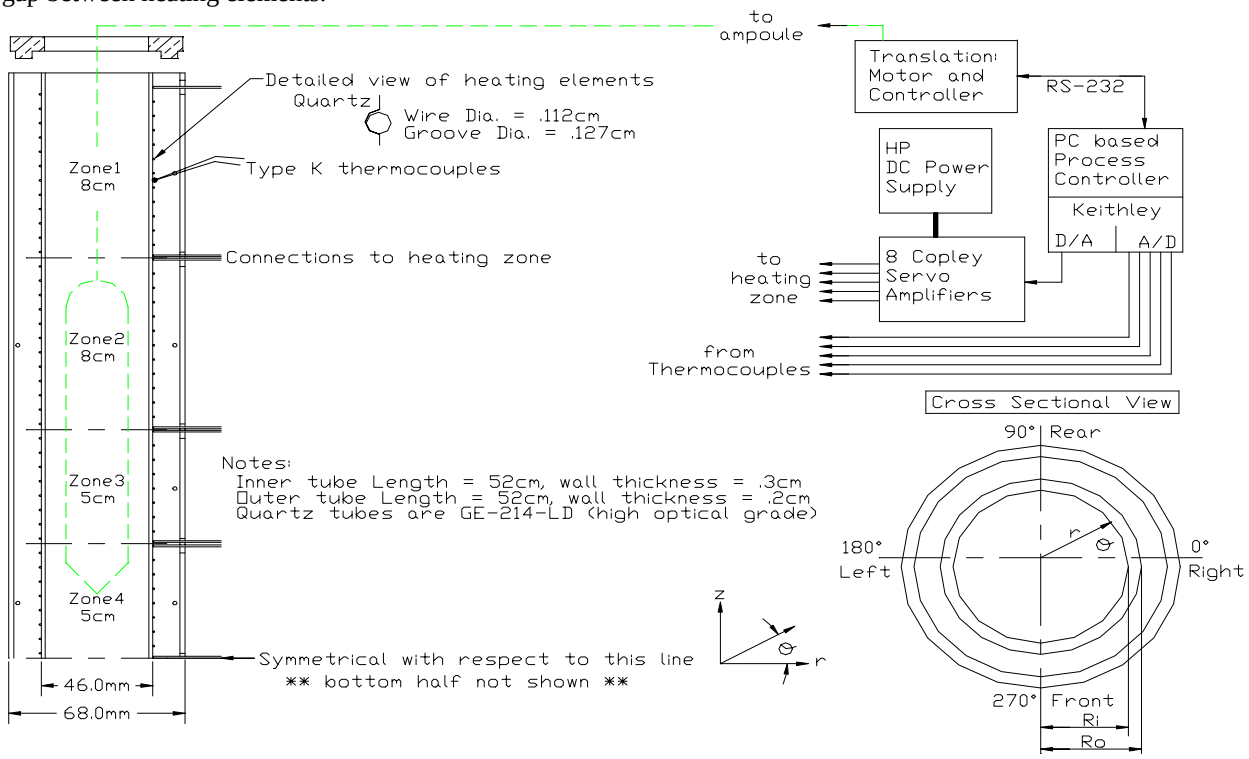

Figure 1 - Schematic diagram of the furnace with ampoule and its associated hardware, cross sectional view shows location for wall temperature measurements.

The optimum length of the zones is selected to allow maximum power input for a given coil in order to achieve a certain temperature range. Whereas, the optimal pitch of the heater wires for each zone is selected such that maximum visibility is achieved through the heating coils. This feature makes the furnace useful for flow visualization studies as demonstrated by Lan et.al. [11]. The heating zone lengths necessary to meet our criteria are as follows: top and bottom zones of Z_1=7.5cm, Z_2=8.0cm and Z_7=8.0cm, Z_8=7.5cm respectively, and equal lengths of the inner four zones: $Z_3 = Z_4 = Z_5 = Z_6 = 5.0$ cm. This heating arrangement can provide an operating range from 25 ^oC to 750 ^oC and thermal gradients from 2 ^oC/cm to 45 ^oC/cm.

2.2 Temperature Control --- Hardware Implementation

The furnace zone temperatures are measured on the outside wall of the inner quartz tube with K type thermocouples. The thermocouple beads are of 0.5 mm in diameter and they are housed inside the small blind holes which are machined on the outside surface of the quartz tube. The positioning of thermocouples in this fashion insures that the beads are at equal distance from the centerline of the furnace. Therefore, the temperatures are controlled at equidistant locations with respect to the centerline. The measured temperatures are cold junction compensated and digitized by a Keithley analog to digital converter. The conversion resolution is 12 bits and, therefore, based on 0 - 1000 ^{o}C temperature range the smallest amount of temperature change that the measurement system can detect is about 0.25 ^{o}C.

The power inputs to heating zones are delivered through eight Copley servo power amplifiers. A 12 bit digital to analog (D/A) card from Keithley supplies a control voltage of 0 - 10 V to each servo amplifier. Since the D/A card is of 12 bits, a minimum amount of voltage change that the D/A card can send to the servo amplifier is about 2.5 mV. This effectively defines the resolution of the control signal. The servo amplifier can provide up to 500 W power to each heating zone. The gain of each amplifier is set to a level such that the (0- 10) V input from the D/A board corresponds to (0 - V_s) Volts where V_s is the supply voltage. There are two Hewlett Packard regulated DC power supplies, connected in parallel and providing up to 8000 W of power to heating zones through power amplifiers. The main advantage of using a DC power supply is the elimination of power supply induced disturbances. These disturbances are inherent characteristics of an AC power supplied furnace. This is due to the fact that there are basically two different ways that one can use to deliver the power from an AC source to the furnace in a regulated manner. One way is based on changing the power activation point within each cycle of the AC voltage. Since this implies a sudden current change to the heater within each cycle, the resulting effect is electrical noise due to inductive nature of the heating element. The second type of systems use zero crossing and duty cycle modulation where the duty cycle is defined as the ratio between the (power on) time to (power on + plus power off) time. Under this system, the heating zone effectively operates under ON-OFF control and if the duty cycle is small this ON-OFF type power regulation introduces its own disturbance into the thermal dynamics. The DC power supply completely eliminates the power supply induced disturbances. A schematic that shows the main features of the hardware is also given in Figure 1.

2.3 Temperature Control --- Software Implementation and Thermal Model

The temperature of each zone is controlled by a self-tuning PI (Proportional - Integral) control algorithm. There are two kind of disturbances that require the self-tuning control action. The first group is due to the motion of the ampoule and the interface which change the thermal dynamics of the heating zone because of changes of thermal inertia within the zone during motion. The second disturbance is caused by the inevitable zone to zone heat exchange since the heating zones are not thermally insulated. At each sampling instant the temperature control algorithm first updates the thermal model of the zone so that the current input output data fit the model in a least squares sense. We assume the following dynamic model for the purpose of controller design

$$T(t) = A.T(t-1) + B.u(t-1) + e(t) \quad (1)$$

Where $u, T \in R^8$ are the process inputs and the measured zone temperatures respectively and $e(t) \in R^8$ indicates the inevitable zone to zone thermal interaction on the temperatures. The matrices $A, B \in R^{8x8}$ define the thermal dynamics of the system. The process input is determined by the temperature controller and it is the energy flow into eight heating zones, i.e., $u=(u_1,u_2,\ldots,u_8)^T$. Once the thermal model is updated, the parameters of the PI controller is modified in order to take into account the most recent changes in thermal dynamics. The model updating is based on the multivariable Least Squares criterion, i.e., at each sampling instant the model matrices A and B are updated such that the sum of squares of the residuals are minimum, i.e., the following identification performance index is minimum

$$V_{ID} = \mathrm{trace}\{\arg_{\hat{A},\hat{B}} \min[\sum_{k=1}^{t} \hat{e}(k).\hat{e}^T(k)]\}, \quad (2)$$

where the residual of the model is given by

$$\hat{e}(k) = T(t) - \hat{A}.T(t-1) - \hat{B}.u(t-1). \quad (3)$$

The modification of the PI control parameters is based on the eigenvalue placement whereby the PI control parameters are changed such that the control system generates the fastest corrective response to the disturbances without causing overshoot or undershoot in the zone temperature. The details of the algorithm can be found in [12].

3.0 ENERGETICS AND MEASUREMENTS OF THERMAL PROFILES

3.1 Relationship between Set-points and Measured Temperatures

A given temperature profile in the furnace is established by setting eight discrete temperatures, T_1, T_2, T_3, …..T_8, at the midpoint of each zone on the outer surface of the inner cylinder. Previous designs in which holes were drilled along the axis of the inner tube suffered from significant heat loss which prevented a uniform thermal field inside the furnace. When a given zone, Z_i is activated at a temperature T_i, the control system sets-up a heat flux distribution, $q''(\theta, z)\ at\ r = Ro$ on the outer surface of the inner cylinder. Some of this heat is lost and the remaining is transmitted inside the furnace which results in thermal equilibrium due to contributions of the heat flow modes, namely, conduction, convection, and thermal radiation. Since the temperature along the inside wall (r = Ri) can be readily measured, the imposed boundary condition may be denoted by the temperature distribution $T = T(r = R_i, \theta, z)$ instead of the heat flux. In order to ascertain the relationship between set-point temperatures and the temperatures inside the furnace, we use a calibrated NIST-Standard type S thermocouple to measure the thermal profile. Since we have air inside the furnace, fundamentally the temperature profile is influenced by buoyancy induced flows due to density gradients, this problem may be posed as follows:
For a set-point temperature, T_i, which establishes a surface temperature

$$T=T(\theta, z) \text{ at } r=R_i, \quad (4)$$

along the inside wall of the inner cylinder for a given zone Z_i, buoyancy induced flows will ensue inside the furnace when the axial heat loss along the wall creates unstably stratified air layers. This heat loss causes a gaussian-like temperature distribution for the individual inner zones of the furnace Z_2-Z_7. The density of air, a homogeneous fluid, is a function of temperature and pressure,

$$\rho = \rho\left(P, T \right). \quad (5)$$

Within first order approximation the effect of pressure may be neglected so that,

$$\rho = \rho o + \frac{\partial \rho}{\partial T}\left(T - To\right) + \frac{1}{2!}\frac{\partial^2 \rho}{\partial T^2}\left(T - To\right)^2 + ... \quad (6)$$

The subscript o indicates a mean value, due to small variation of the density with temperature, second order derivatives and higher may be neglected. Regions in which the density field becomes unstably stratified, due to an adverse density field variation from equation 6, will give rise to a flow field which satisfies the conservation of mass, balance of momentum, and conservation of energy as follows:

$$\nabla \bullet \vec{V} = 0 \quad (7)$$

$$\rho_0 \frac{D\vec{V}}{Dt} = -\nabla P + \mu \nabla^2 \vec{V} + \rho\ \vec{g} \quad (8)$$

$$\frac{DT}{Dt} = a\ \nabla^2 T. \quad (9)$$

$\vec{V}$ represents the flow field, $\vec{g}$ is the gravitational acceleration, μ and α are the dynamic viscosity and thermal diffusivity of the fluid. The above equations represent an incompressible flow in which the density variation occurs only in the body force term, hence a Boussinesq fluid. The density field variation in equation (6) gives the coupling between the energy equation (9) and the momentum equation (8). The solution to this problem can be determined numerically to obtain the temperature field inside the furnace,

$$T=T(r, \theta, z, t), \quad (10)$$

as a predictive tool for a prescribed boundary condition. Alternatively, the temperature field can be measured to obtain the solution. In our case we measured the temperature field and found that azimuthal symmetry, i.e. T(r,z), in the gradient region for linear temperature profiles is a good approximation. Even though, there is a slight radial

dependence, the temperature profile at the centerline, T=T(z) at r=0, gives a good indication of the temperature gradient.

3.2 The elements of thermal profile

The measured centerline thermal profile consists of a functional combination of the profile of individual zones. Figure 2, shows the corresponding thermal profile for a set point temperatures of T=373 ^{o}C applied at each zone individually, the origin of the coordinate system is at the top of the furnace. These profiles correspond to one zone in operation, while keeping the other zones off. Since zone 1 is near the top, the heat loss near the top of the quartz tube is minimal. There is a local temperature maximum in zone 1 which decreases exponentially toward the bottom of the furnace. In contrast, note that heat loss, for all the zones, along the axial direction towards the top of the furnace increases as the zone distance from the top of the furnace increases. This effect of heat loss is augmented by the Rayleigh-Taylor instability which occurs due to unstable air density stratification, which is shown by the scatter of data near the top region, illustrated more clearly for zone 6. This convective flow situation denoted by $\vec{V}$ in equation (8) occurs because the air density increases, above the location of the maximum temperature, for example zone 4; this provides a situation where a heavy air layer lies on top of a lighter layer which gives rise to a convective flow field. The scatter of the data as shown in zone 6 is attributed to this convective instability. On the other hand, note that toward the bottom of the furnace the temperature profile is smooth; this is because as the temperature decreases the lighter fluid air elements overlays the heavier elements which provide a stable situation. Thus, there is no convective flow. The gaussian-like wall temperature distribution as shown in our furnace has similar effect on driving buoyancy induced convection as the case of a heat source at the bottom of the furnace [13] in which the walls would either have a linear imposed temperature gradient or be insulated.

The temperature profiles in Figure 2 showed the one dimensional (1-D) behavior of the thermal field at the centerline, however, for a given axial location (z) it is likely that there exists 3-D thermal surfaces in the (r,θ) plane. In order to investigate this likelihood, in addition to the centerline we also probed the inside wall of the furnace to permit a 3-D reconstruction of the temperature field. In contrast to the measurements in Figure 2 which used an AC based power system (kanthal wire diameter .125cm), we switched to a DC power supplied furnace with different Kanthal heating wire diameter .081cm, hence different resistance. Using the same set-point as before 373 ^{o}C, we obtained the same trends in zone 4 shown in Figure 3, however, the magnitude of the response temperature in the furnace varied. The wall temperatures were measured at the z-plane which corresponds to 0^{o} (Right), 90^{o} (Rear), 180^{o} (Left), 270^{o} (Front), respectively as shown in Figure 1. The results show that maximum deviation from the centerline temperature occurs in the neighborhood of the local maximum, which is located at z = 26 cm, of the thermal profile. A 3-D reconstruction shows that the thermal surface corresponds to a skewed paraboloid of

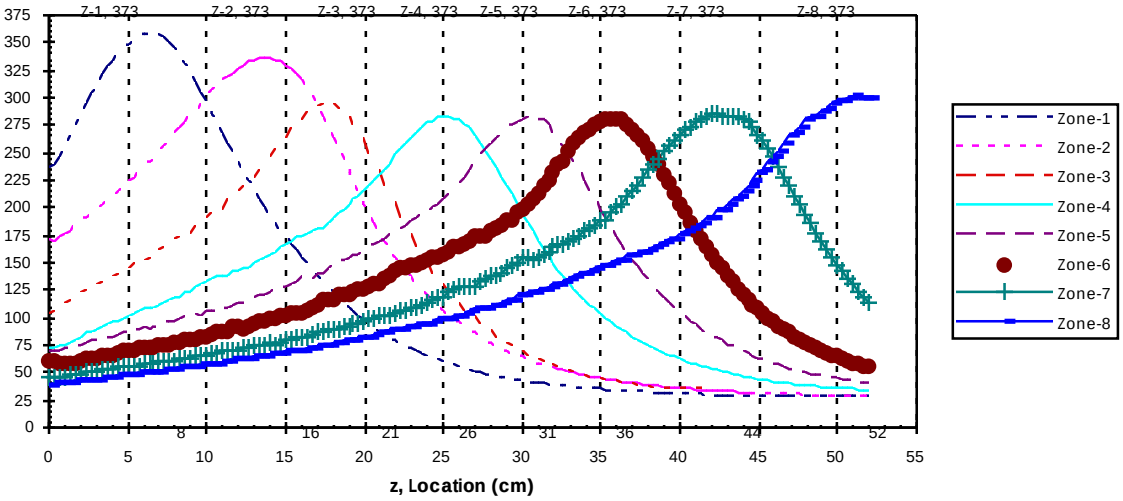

Figure 2 - Thermal profile characteristics of the furnace illustrating the behavior of each zone for the same set-point temperature, T=373^{0}C. Top numerical numbers indicate zone set-point temperatures (^{0}C), bottom numbers on the axis indicate location of boundaries between zones.

revolution at z = 26 cm. Note that near the top of the furnace for example at z < 19 cm, the centerline temperature becomes higher than the wall temperatures. This trend is attributed to intense convective motion as we had discussed earlier. In contrast for z > 30 cm in which there is no convective motion, the centerline temperature is approximately the same as the wall temperatures. The isothermal surface for the location z = 35 cm would correspond to a skewed hemisphere, note that the centerline temperature is greater than most of the wall temperatures for this region. Much of the skewdness in the 3-D representation stems from the helical path of the heating wire which will inevitably cause local temperature nonuniformity on the wall of the furnace. Since the majority of practical thermal profiles for crystal growth is obtained by fixing a hot and a cold zone similar to the region z > 30 cm, the centerline temperature profile would give a good representation of the thermal gradient. Though, we have shown the furnace response when a single zone is activated, the effect of activating two or three zones simultaneously using the same set-point is to broaden the peak of the thermal profile such that a flat isothermal region is obtained.

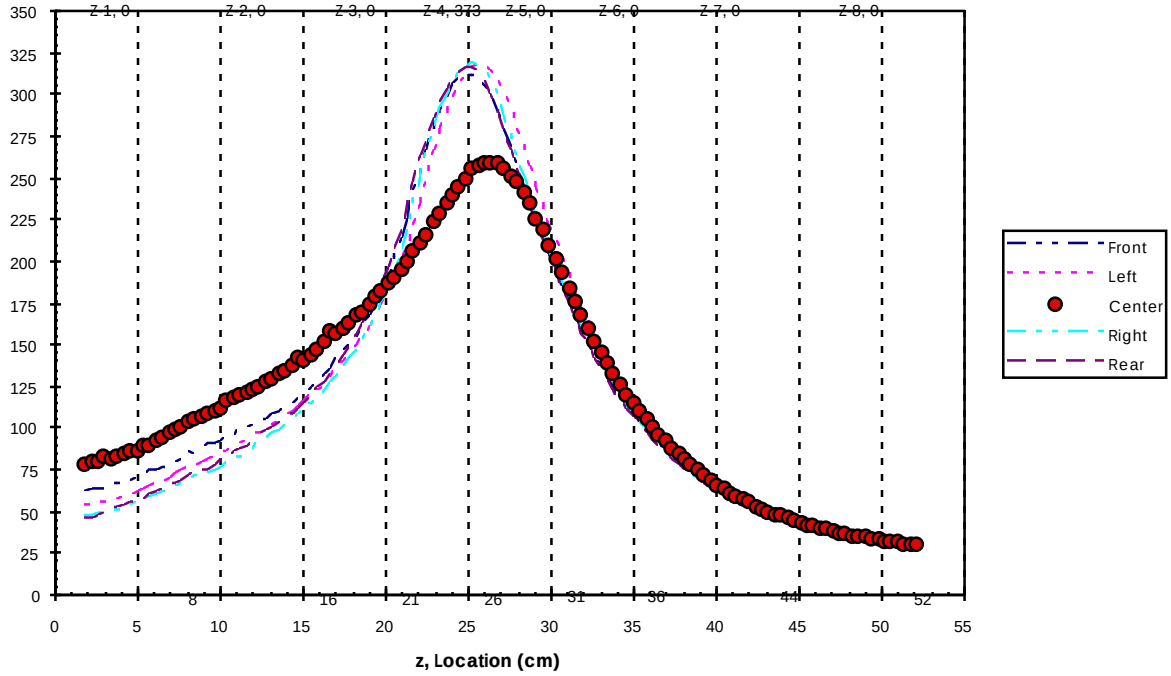

Figure 3 - Comparison of wall and centerline temperatures when only zone 4 is activated for a set-point of 373^{0}C. Set-point temperatures of 0 ^{0}C indicate no power supplied to indicated zones.

Given the individual performance of the various zones, operation of all the zones in synchronization results in nearly isothermal conditions over a segment, 25cm ≤ z ≤ 35cm, of the furnace shown in Figure 4. All the zones were set to the same temperature for each case, slight adjustments can be made to achieve the desired level of isothermality. Crystal growth under practical conditions requires specific thermal profiles, we show various profiles measured at the centerline as well as the wall to give an indication on how well the furnace projects the imposed thermal boundary conditions. An example of a linear thermal gradient is shown in Figure 5. This thermal gradient is necessary for the growth of crystals via directional solidification. The wall temperature gradient in the region of interest 16 cm ≤ z ≤ 25 cm is approximately the same as that of the centerline (20 ^{o}C/cm) The growth of crystals by physical vapor transport necessitates a thermal profile with a "hump" shown in Figure 6. This case illustrates that maximum deviation of the thermal gradient occurs in the region of the "hump", 20cm ≤ z ≤ 28 cm. The centerline temperature gradient for that region is 17^{o}C/cm, whereas the average wall gradient is 31^{o}C/cm. As we had discussed earlier, some applications necessitate localized heat transfer in one direction, the multiple gradient shown in Figure 7 is an alternative for obtaining the same effect as insulation while preserving the transparency of the furnace. The isothermal region occurs for 23 cm ≤ z ≤ 29 cm, and centerline thermal gradients of 25 ^{o}C/cm and 20 ^{o}C/cm corresponding to the regions 15 cm ≤ z ≤ 20 cm and 30cm ≤ z ≤ 39cm respectively. There is good agreement between the wall and centerline temperatures for those regions.

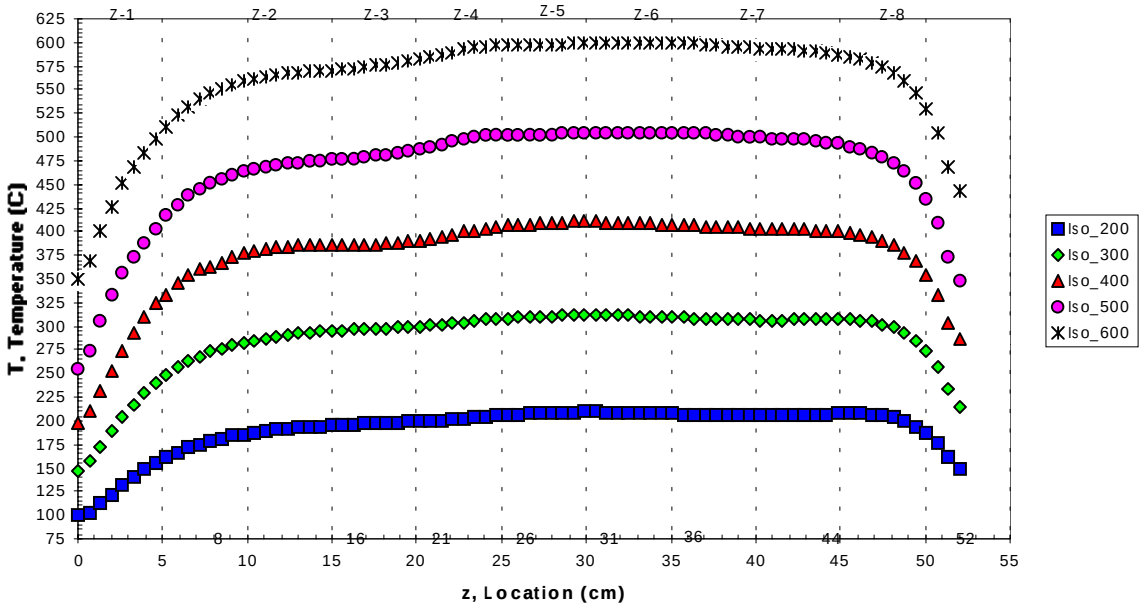

Figure 4 - Illustration of nearly isothermal profiles when all zones are set to the same temperature.

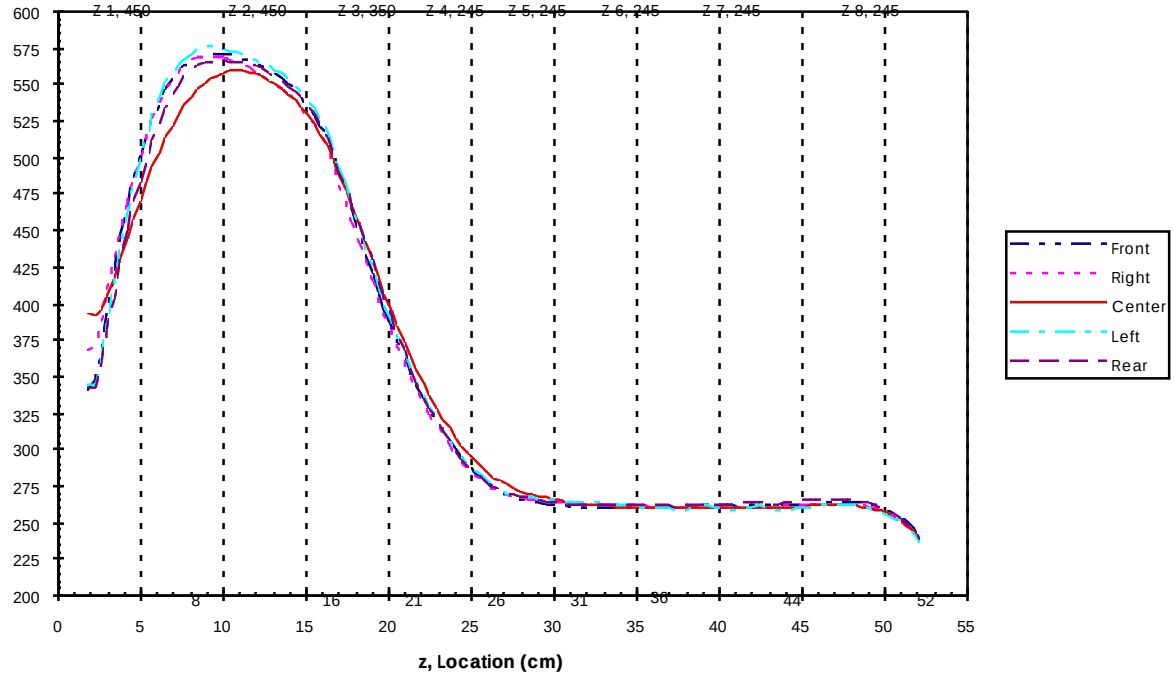

Figure 5 - Thermal profile used for crystal growth by directional solidification, dT/dz = 20 ^{o}C/cm in the region 16cm $\leq$ z $\leq$ 25cm.

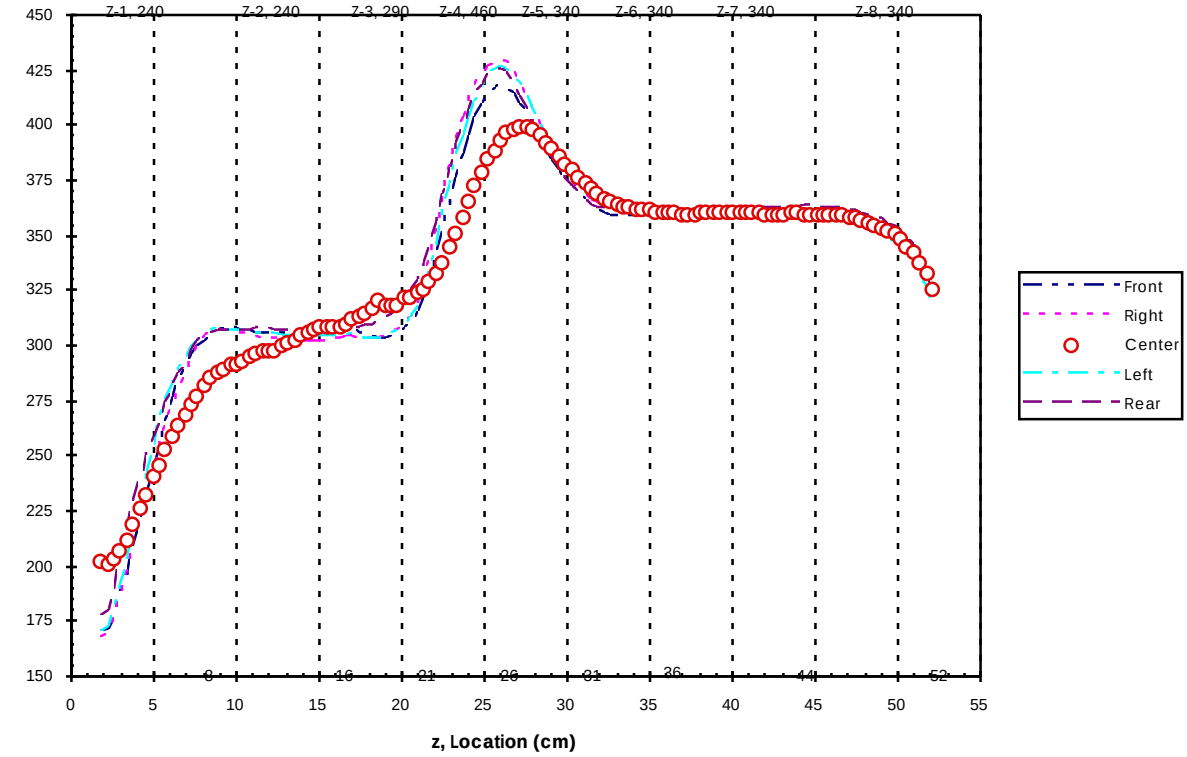

Figure 6 - Nonlinear thermal profile used for crystal growth by physical vapor transport, local temperature gradient at the centerline in the vicinity of 22cm $\leq z \leq$ 27cm is 17°C/cm.

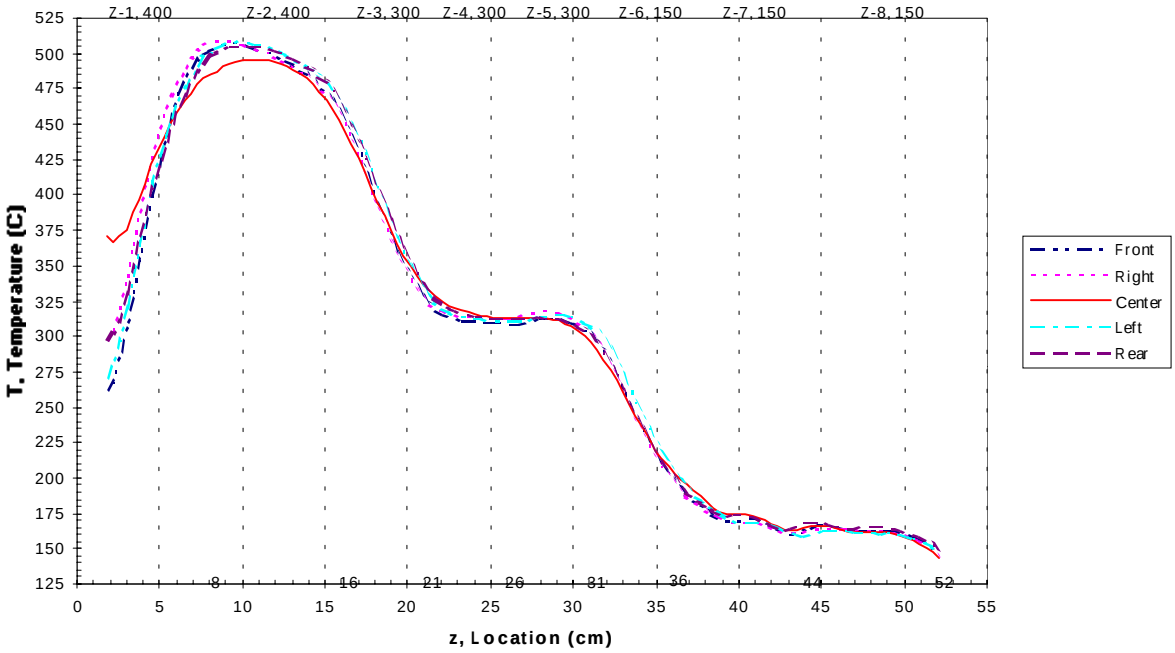

Figure 7 - Illustration of multiple gradient capability with isothermal region.

3.3 Effect of Ampoule on Thermal Profile

We have discussed in detail the furnace performance under no load conditions. The self-tuning temperature control is designed to account for zone to zone interactions. However, the thermal profile is preserved even with the presence of an ampoule for crystal growth. To show the response of the furnace under load conditions, we use the same condition as shown in Figure 5 for the linear thermal gradient. Note that the presence of an ampoule damps convective flows in the furnace. Figure 8 shows the measured thermal profile on the surface of an ampoule, 1.7 cm diameter and length 35.0 cm, containing lead bromide with a melting point of 373 ^{0} C. Comparison of the location of the solid-liquid interface to that indicated by the thermal profile shows reasonable agreement. This provides a calibration point for our thermal profile measurements. The result indicates that the control system accounts for thermal load conditions. Thus the thermal gradient projected by the furnace under no load conditions measured at the centerline corresponds to the surface input temperature at the ampoule wall. This implies that predetermined boundary conditions can be used as input to the furnace to study the dynamics of crystal growth. The ability of the self-tuning control system of the furnace to tailor thermal profiles represents an innovative concept that will find commercial applications for optimizing crystal growth conditions.

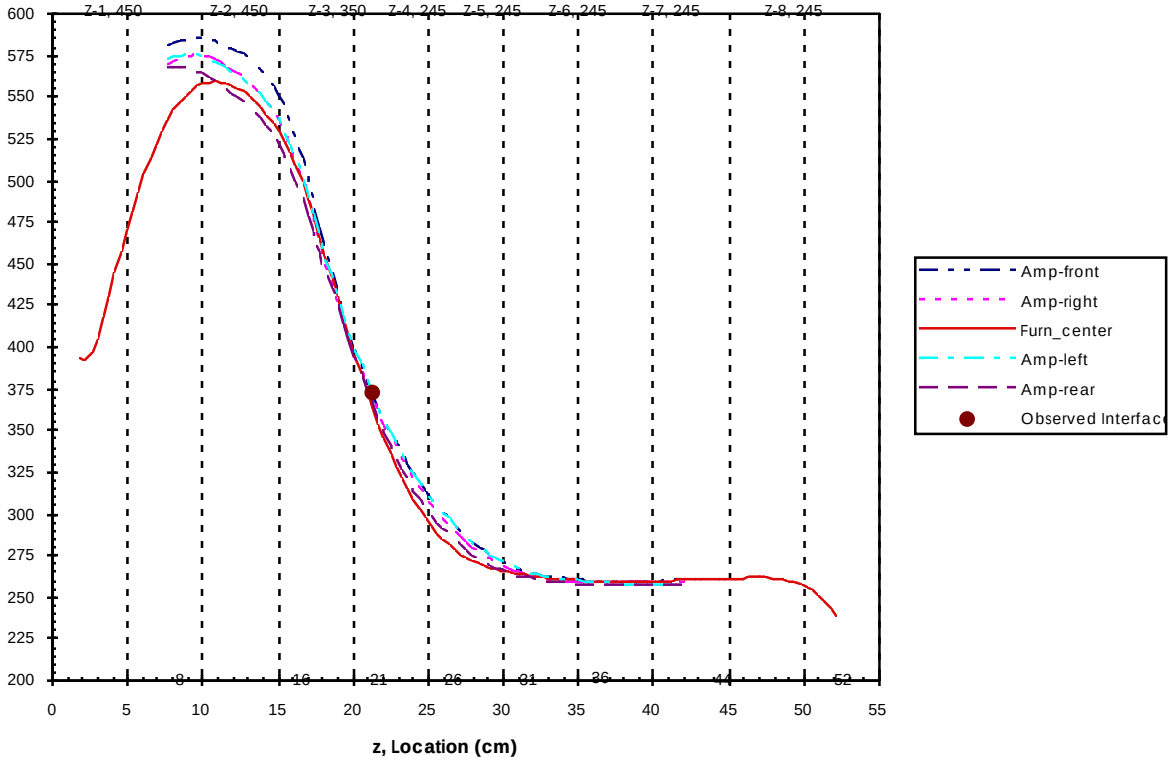

Figure 8 - Comparison of projected temperature profile under load conditions due to presence of ampoule filled with lead bromide, to no load conditions represented by centerline profile of the solid curve, $dT/dz = 20^0$C/cm $16\text{cm} \leq z \leq 25\text{cm}$. Location of observed solid-liquid interface at the melting point of lead bromide, 373^0C, serves as a calibration point (see legend) for the system.

3.4 Thermal Mapping

Having established the relationship between the wall and centerline temperature profile in the furnace, and gained confidence on the magnitude of the measured temperatures through calibration with the known melting point of lead bromide ($PbBr_2$), we investigate the ability of a thermal probe to measure the thermal field at an arbitrary z-plane inside the furnace. This thermal probe, shown in Figure 9, consists of three cylindrical boron-nitride disks which hold 13 rods with imbedded thermocouples. The three disks have a diameter of 3.3 cm and are located 4.5 cm,

28.5 cm, and 52.5 cm from the tip of the thermocouples which are placed inside alumina sheaths. The layout of the thermocouple placement is similar to concentric cylinders with radii r1= .66cm and r2=1.32cm . The thermocouple at the centerline is a calibrated NIST standard type S, whereas the remaining thermocouples are regular calibrated type K thermocouples. The accuracy of the probe was checked at the boiling point of water at atmospheric pressure and showed that all readings were within $\pm$ .3^{o}C. The thermal field inside the furnace is measured by translating the thermal probe assembly through the furnace at a rate of .35 cm/min using a Compumotor Model 172 indexer. This translation speed is set slow enough in order not to interfere with the measurement of the thermal field dynamics.

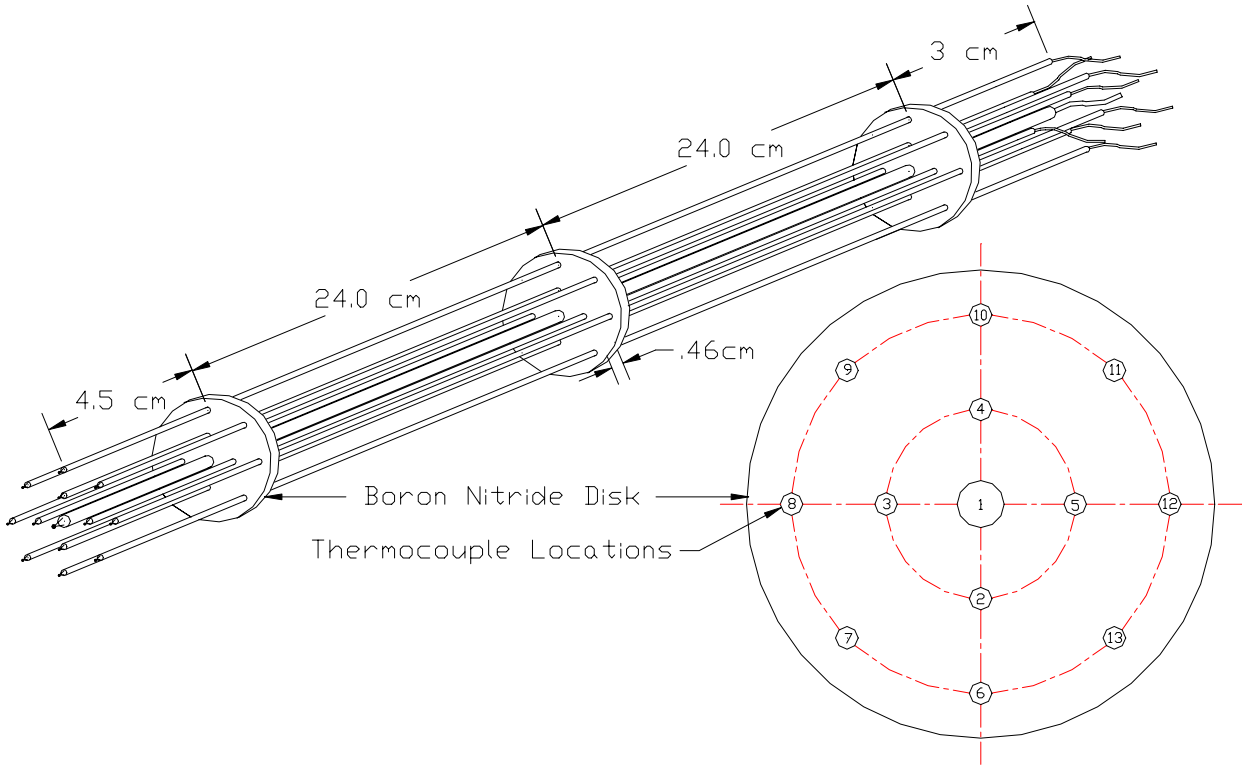

Figure 9 - Thermal probe assembly consisting of 13 rods and cross section of boron nitride disk showing thermocouple locations, center rod O.D. = .17cm, all remaining rods O.D. = .08cm.

For comparison basis, we use the same temperature settings as shown in Figures 3 and 4. The results shown in Figures 10 and 11 indicate that even though the trends of the thermal profile are similar, there exist differences in the magnitude of the temperature measured using the thermal probe. For example, Figure 10 indicates that the centerline temperature is approximately 50 ^{o}C greater than that measured in Figure 3 using a single probe at the location z = 26 cm. For the region $0 < z < 26$ cm , the measurements provide insight into the penetration of the convective instability from the point where the temperature is maximum, z = 26 cm. The measurements indicate that these fluctuations extend to approximately 3 cm beyond the maximum temperature point. In comparison, the region $26 \leq z \leq 52$ cm shows a smooth temperature distribution as before. In contrast, the centerline temperature profile for the thermal gradient of 20 ^{o}C/cm, Figure 11, shows a difference of approximately 25 ^{o}C at z = 21 cm in comparison to the single probe measurement. In both cases, measurements made with the thermal probe indicate higher temperature at the centerline even though a standard thermocouple was used for both cases at the central location.

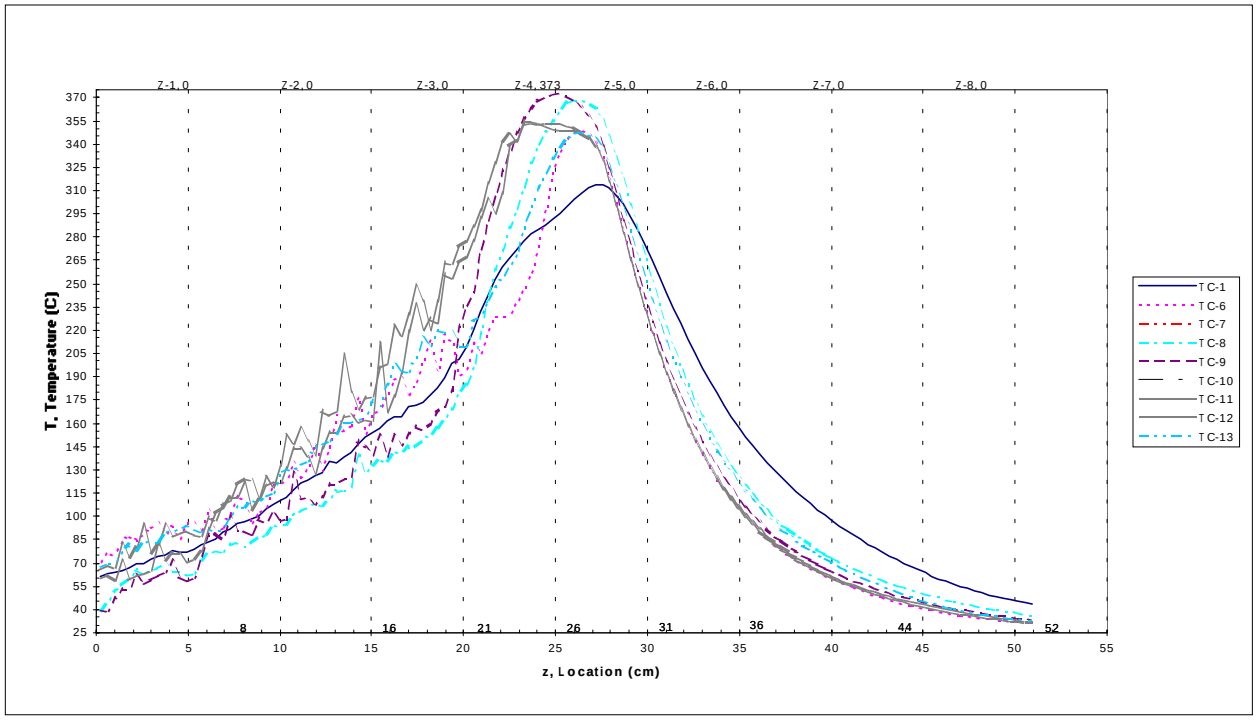

Figure 10 - Thermal profile corresponding to the same settings as in Figure 3 measured using the thermal probe. The temperatures at locations 2,3,4,5 are not shown in order to preserve the clarity of the figure.

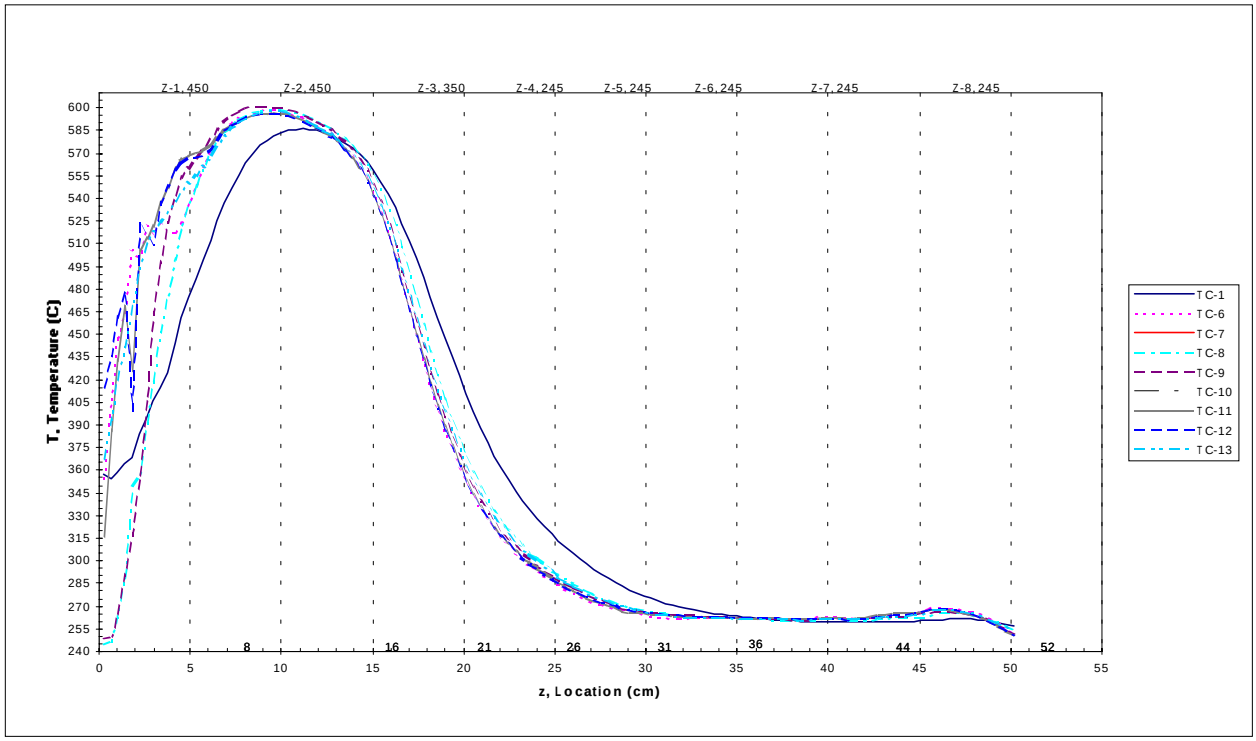

Figure 11 - Thermal profile corresponding to the same settings as in Figure 4 measured using the thermal probe.

The higher temperature reading of the probe is mainly attributed to thermal radiation exchange between the probe assembly and the inner surface of the quartz tube. Prior temperature measurements show that a single rod is not sufficient to contribute to thermal radiation effects, however, a probe assembly consisting of 13 rods absorbs and emits sufficient thermal radiation to increase the local temperature inside the furnace. Quartz transmits in the wavelength range of $.17\mu m \le \lambda \le 2.7\mu m$ [14], and absorbs thermal radiation outside of that range. The maximum wavelength of thermal radiation emitted by the source (Kanthal wires) may be estimated from Wien's displacement law,

$$\lambda_{max} T = 2897 \ \mu m \ ^{o}K . \quad (11)$$

For temperatures in the range of 300 ^{o}C to 600 ^{o}C , the corresponding maximum wavelength lies at $\lambda_{max} = 5.05\mu m$ and $\lambda_{max} = 3.32\mu m$. This implies that local thermal equilibrium inside the furnace is achieved through the net exchange of emission and absorption of thermal radiation for that temperature range. The agreement between the measured temperature which corresponded to the location of the solid-liquid interface of lead bromide, Figure 8, stems from the fact that $PbBr_2$ transmits in the range of .35 to 30 μm, the absorption of thermal radiation was negligible thus the local temperature did not increase. However, since the probe assembly is opaque, it absorbs and emits thermal radiation in the long wavelength region which is trapped by the quartz cylinder. The thermal energy of the system increases, thus increasing the local temperature. A secondary effect causing the higher temperature readings is the fact that the thermal probe assembly changes the convective flow field. In fact, in comparison to the single probe configuration, the convective flow field is significantly blocked due to the boron-nitride disks.

The use of the thermal probe allows reconstruction of isothermal contours and surface for a given z-plane. The isothermal contours give an indication on regions in the furnace in which the temperature field is uniform. Temperature contours were analyzed for various axial planes, the results for practical conditions such as Figure 11 show that in the neighborhood of $0 \le r \le 6cm$ the thermal gradient is approximately linear. This is illustrated in Figure 12 which shows a projection on Cartesian coordinates, for the axial plane z = 20 cm. Since we only measure the temperature at 13 points, the results show somewhat course contours; thus the thermal surface is not shown. However, these measurements are sufficient at this stage to give an indication on trends of the temperature field. This method can potentially be used to map the thermal surface, however, a large number of thermocouples is needed for increased accuracy.

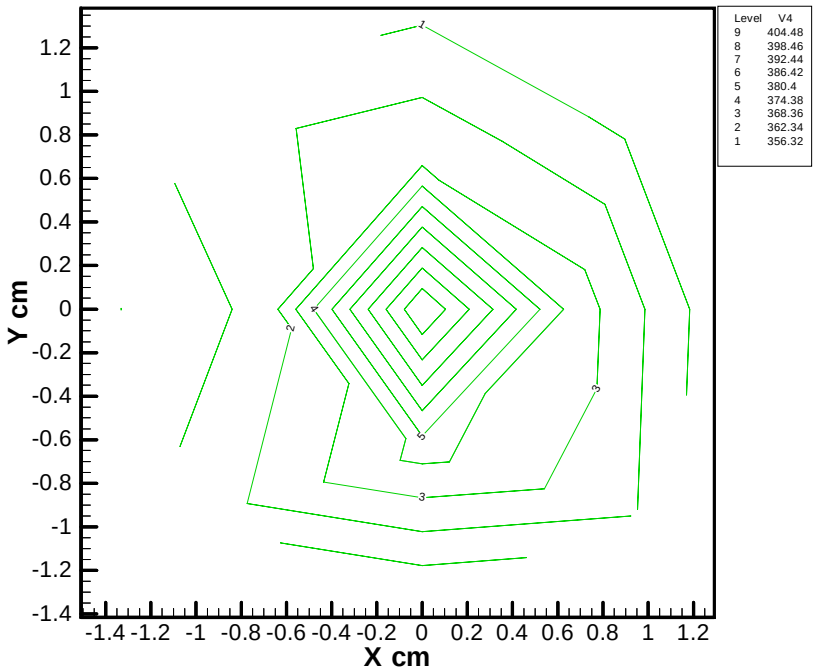

Figure 12 - Temperature contours for the thermal gradient of 20 ^{o}C/cm at the axial plane z = 20 cm.

3.5 Quantification of Thermal Convection

The characteristics of thermal convection is investigated by considering the thermal history at the centerline location for several points in the furnace, with the initial point z = 2 cm in increments of approximately 5 cm . These measurements are made using a single rod, thus Figure 3 may be used as a reference instead of Figure 10. The time history of the temperature field in the region 2 cm $\leq$ z $\leq$ 27 cm indicates fluctuations on the order of 1 to 2 ^{o}C. An example of the time history for the location z = 16 cm, shown in Figure 13, indicates an aperiodic fluctuation of the temperature field. The time dependence is assumed to be represented by a stationary process; this implies that the time averaged properties such as the mean and variance are independent of time, in essence the behavior of the temperature fluctuations do not change for much longer time intervals. The ensemble average for this stationary process is assumed equal to the time average, hence the process is ergodic. The mean of the temperature is estimated as $\bar{T}$ = 178.86 ^{o}C and its standard deviation σ = 1.71 ^{o}C. Quantification of the aperiodicity may be obtained from the power spectral density,

$$P_T(f) = \frac{1}{R}\left| \int_0^R T(t) e^{-j2\pi ft} dt \right|^2 , \quad (12)$$

in which R denotes the time interval of the data. The result in Figure 14 indicates a broadband power spectrum, which is indicative of a chaotic condition or soft turbulence of the buoyancy induced flow inside the cylinder. In contrast, note that the time history at the location z= 32 cm in Figure 15, indicates a fairly steady temperature, the mean is $\bar{T}$ = 146.5 ^{o}C, and standard deviation σ = .21 ^{o}C. These fluctuations are caused by measurement error and also represents the performance of the controller. This shows conclusively that there is no convection in this region, as we had hypothesized earlier.

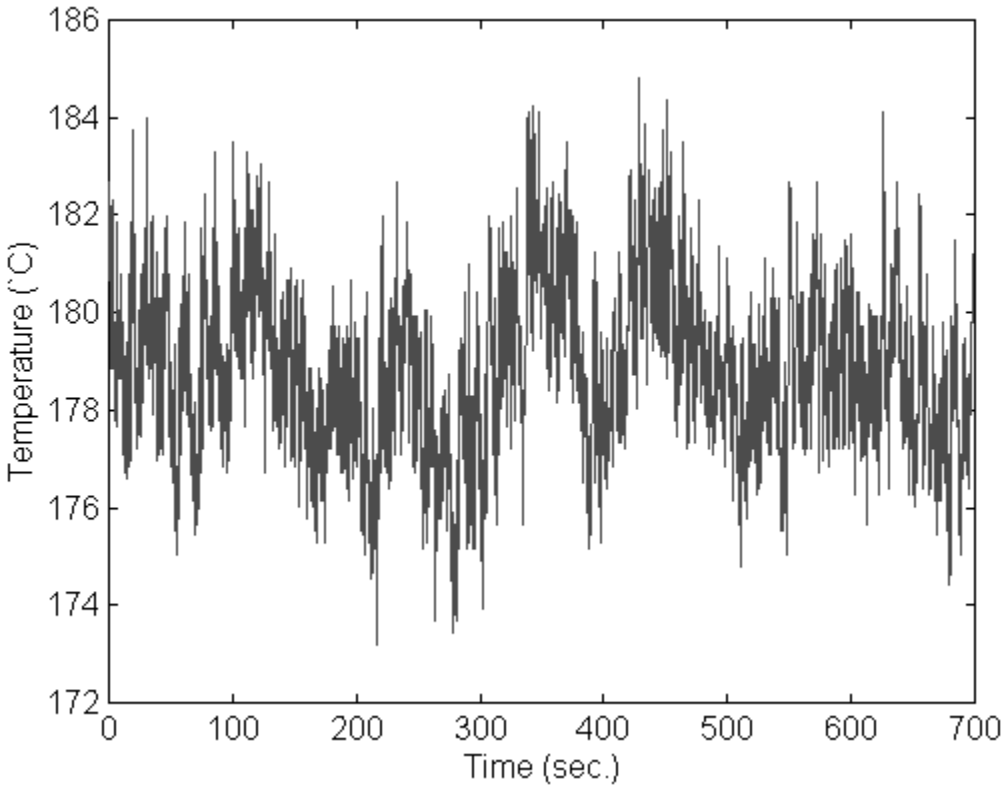

Figure 13 - Time history of temperature field at centerline location for z =16cm when zone 4 is activated at T =373 ^{o}C.

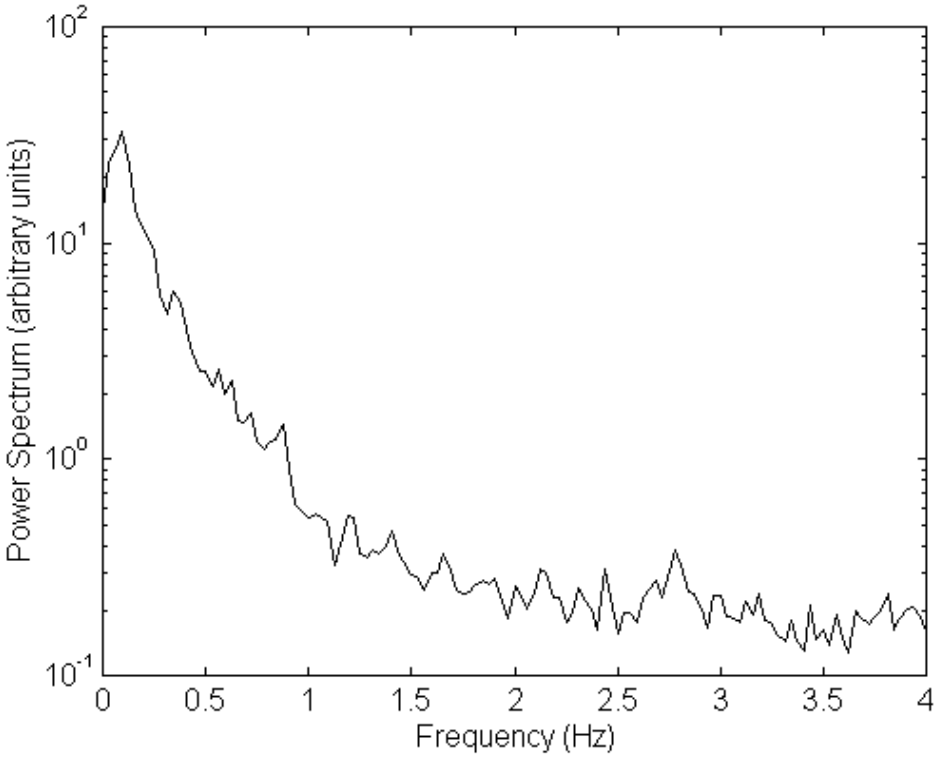

Figure 14 - Power spectrum density corresponding to thermal history at z = 16cm.

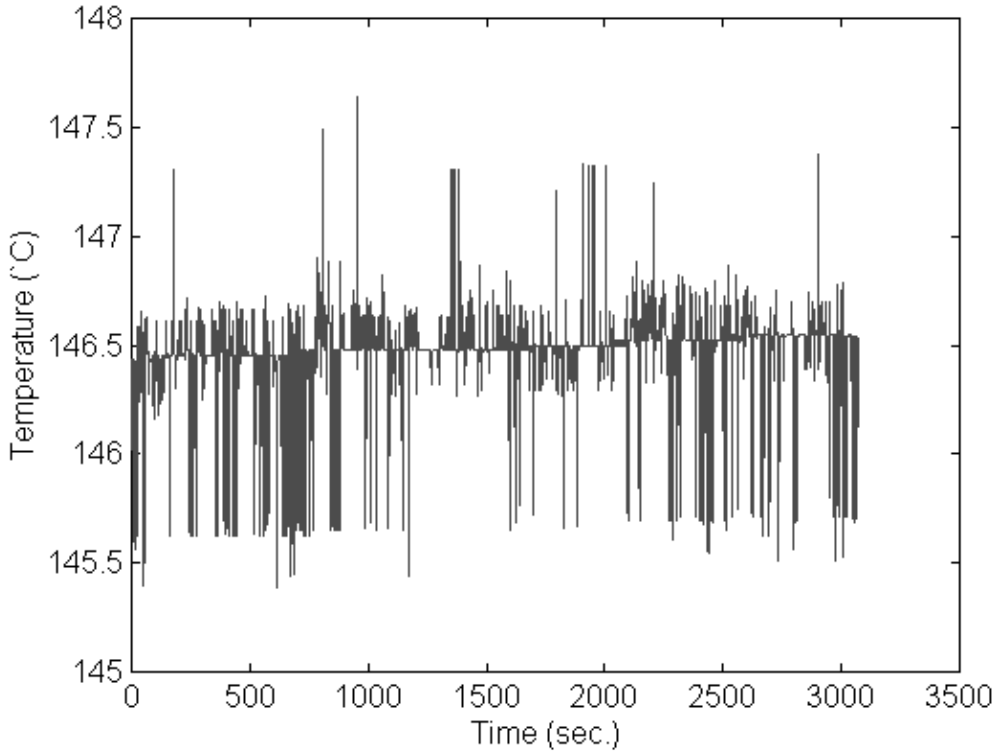

Figure 15 - Time history of temperature field for z = 32 cm illustrating typical temperature fluctuations in the quiescent region.

4.0 SUMMARY AND CONCLUSIONS

We have introduced an innovative concept of a transparent multizone furnace which uses a self-tuning temperature control system for the commercial application to crystal growth. This furnace operates in the temperature range of 25 - 750 ^{o}C . The self-tuning control accounts for zone to zone thermal interactions. The control system adjusts for thermal load, thus thermal profiles can be tailored prior to crystal growth and thermal gradients in the range of 2 ^{o}C/cm to 45^{o}C/cm can be obtained. The operation of the furnace is based on the set-up of eight discrete temperatures over eight zones which result in a functional combination of heat flux distribution whose response is quantified from temperature profile measurements. The combination of the temperature profiles for a given set-point temperature is shown to give temperature profiles of technological interest for the growth of crystals. These profiles include a range of thermal gradients for directional solidification applications, growth by vapor transport techniques, as well as multiple gradient applications. The innovation of the multizone crystal growth furnace is suited for crystal growth of a wide class of materials including, acousto-optic optoelectronics, photonics, low temperature semiconductors and organic materials. The hallmark of this furnace technology is its transparency and its ability to deliver precise thermal profiles.

5.0 REFERENCES

1.)Fu, Ta-Wei, Wilcox,W., "Influence of Insulation on Stability of Interface Shape and Position In The Vertical Bridgman-Stockbarger Technique," Journal of Crystal Growth, 48, pp. 416-424, 1980.

2.)Ravishankar, R.S., and Fu, T.W. "Mathematical Modeling and Parametric Study of Heat Transfer in Bridgman Stockbarger Growth of Crystals," Journal of Crystal Growth, 62, pp. 425-432, 1983.

3.)Chin, Lih-Yen, Carlson, F. "Finite Element Analysis of Control of interface Shape in Bridgman Crystal Growth." Journal of Crystal Growth, 62, pp. 561-567, 1983

4.)Chang, Chong E. and Wilcox, W. R. "Control of Interface Shape in the Vertical Bridgman-Stockbarger Technique", Journal of Crystal Growth, 21, pp. 135-140, 1974

5.)Hartman ,E., Schonherr, E. "Determination of Crystal Growth Rates from the Vapor by Relaxation," Journal of Crystal Growth, 51, pp. 140-142, 1981.

6.)E Schonherr, "Phenomenological Description of Crystal Growth From the Vapor" Journal of Crystal Growth, 57, pp. 493-498, 1982.

7.)Clyne, T.W. "Heat Flow in Controlled Directional Solidification of Metals, I Experimental Investigation" ,Journal of Crystal Growth 50, pp. 684-690, 1980.

8.)Clyne, T.W. , "Heat Flow in Controlled Directional Solidification of Metals, II Mathematical model", Journal of Crystal Growth 50, pp. 691-700, 1980.

9.)Batur, C., Sharpless, R.B., Duval, W.M.B., Singh, N.B., Rosenthal, B.N., "Identification and Control of a Multizone Crystal Growth Furnace," Journal of Crystal Growth, 119, pp. 371-380, 1992.

10.)Batur, C., Srinivasan, A., Duval, W.M.B., Singh, N.B.,"Control of Crystal Growth in Bridgman Furnace," Prog. Crystal Growth and Charact., 30, pp. 217-236, 1995.

11.)Lan,C.W., Yang, D.T., Ting, C.C., Chen, F.C.," A Transparent Multizone Furnace For Crystal Growth and Flow Visualization," Journal of Crystal Growth, 142, pp. 373-378, 1994.

12.)Srinivasan A., Batur C., Veillette R., "Projective Control Design for Multi-zone Crystal Growth Furnace", IEEE Transactions on Automatic Control System Technology, Vol. 2., No.2., pp. 142-148, 1994.

13.)Neumann, G., "Three Dimensional Numerical Simulation of Buoyancy-Driven Convection in Vertical Cylinders Heated from Below," Journal of Fluid Mechanics, 214, pp. 559-578, 1990.

14.)Siegel, R., Howell, J.R., "Thermal Radiation Heat Transfer," Mc-Graw Hill Book Company, pp. 146-158, 1981.

APPENDIX A

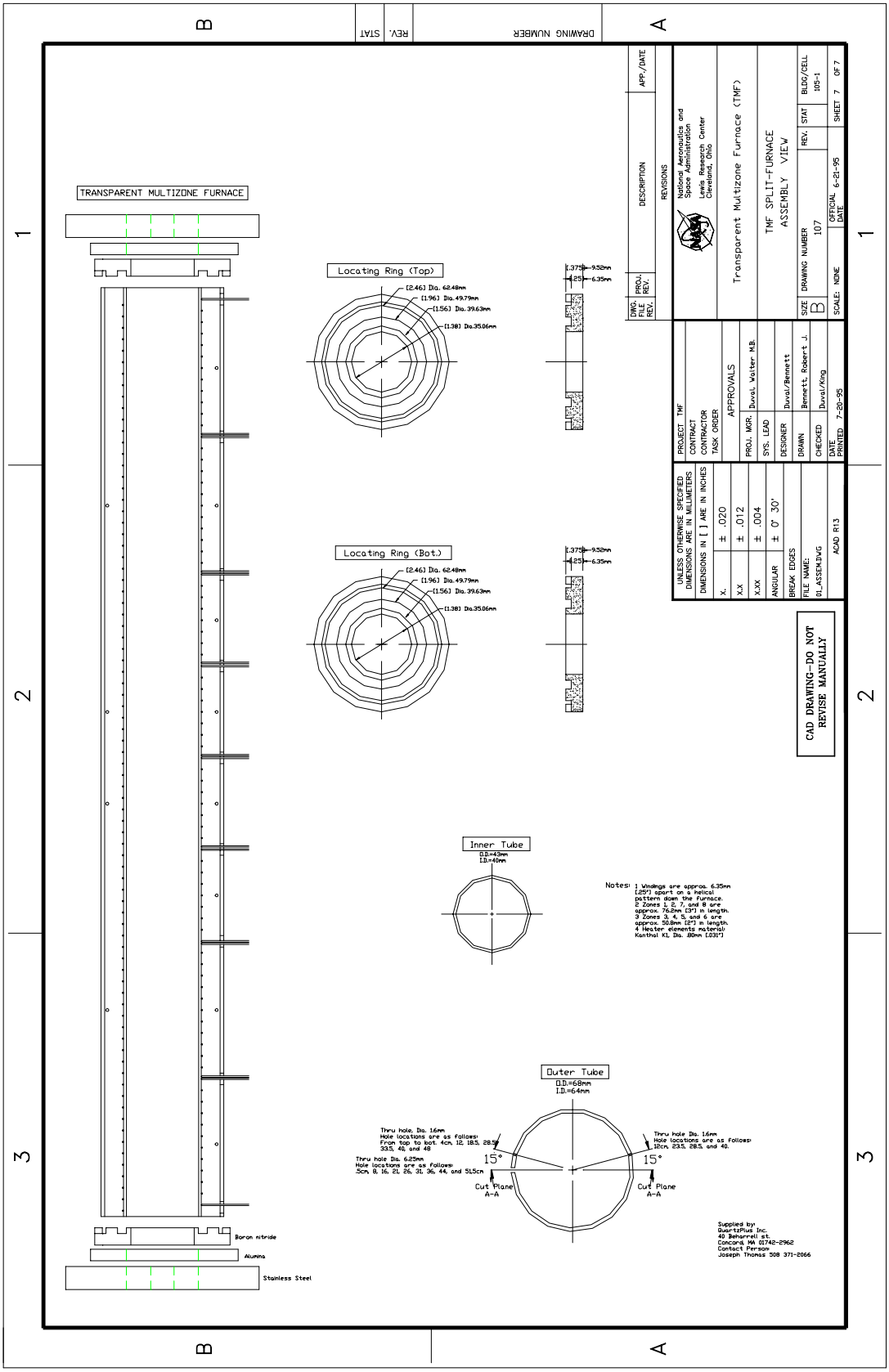
TRANSPARENT MULTIZONE FURNACE
Locating Ring (Top)
(2.46) Dia. 62.48mm
(1.96) Dia. 49.79mm
(1.56) Dia. 39.63mm
(1.38) Dia.35.06mm
.375 9.52mm
.25 6.35mm
Locating Ring (Bot.)
Inner Tube
O.D.=43mm
I.D.=40mm
Notes: 1 Windings are approx. 6.35mm (.25") apart on a helical pattern down the furnace.
2 Zones 1, 2, 7, and 8 are approx. 76.2mm (3") in length.
3 Zones 3, 4, 5, and 6 are approx. 50.8mm (2") in length.
4 Heater elements material Kanthal K1, Dia. .80mm (.031")
Outer Tube
O.D.=68mm
I.D.=64mm
Thru hole, Dia. 16mm
Hole locations are as follows:
From top to bot. 4cm, 12, 18.5, 28.5, 33.5, 40, and 48
Thru hole Dia. 6.25mm
Hole locations are as follows:
5cm, 8, 16, 21, 26, 31, 36, 44, and 51.5cm
Thru hole Dia. 16mm
Hole locations are as follows:
12cm, 23.5, 28.5, and 40.
15°
Cut Plane A-A
Supplied by:
QuartzPlus Inc.
40 Behannell st.
Concord, MA 01742-2962
Contact Person
Joseph Thomas 508 371-2066
Boron nitride
Alumina
Stainless Steel
CAD DRAWING-DO NOT REVISE MANUALLY
DRAWING NUMBER
REV.
STAT
DESCRIPTION
APP./DATE
REVISIONS
PROJ. REV.
DWG. FILE REV.
National Aeronautics and Space Administration
Lewis Research Center
Cleveland, Ohio
Transparent Multizone Furnace (TMF)
TMF SPLIT-FURNACE ASSEMBLY VIEW
SIZE B
DRAWING NUMBER 107
REV. STAT
BLDG/CELL 105-1
SCALE: NONE
OFFICIAL DATE 6-21-95
SHEET 7 OF 7
UNLESS OTHERWISE SPECIFIED DIMENSIONS ARE IN MILLIMETERS
DIMENSIONS IN [ ] ARE IN INCHES
X. ± .020
X.X ± .012
X.XX ± .004
ANGULAR ± 0° 30'
BREAK EDGES
FILE NAME: 01_ASSEM.DWG
ACAD R13
PROJECT TMF
CONTRACT
CONTRACTOR
TASK ORDER
APPROVALS
PROJ. MGR. Duval, Walter M.B.
SYS. LEAD
DESIGNER Duval/Bennett
DRAWN Bennett, Robert J.
CHECKED Duval/King
DATE PRINTED 7-20-95

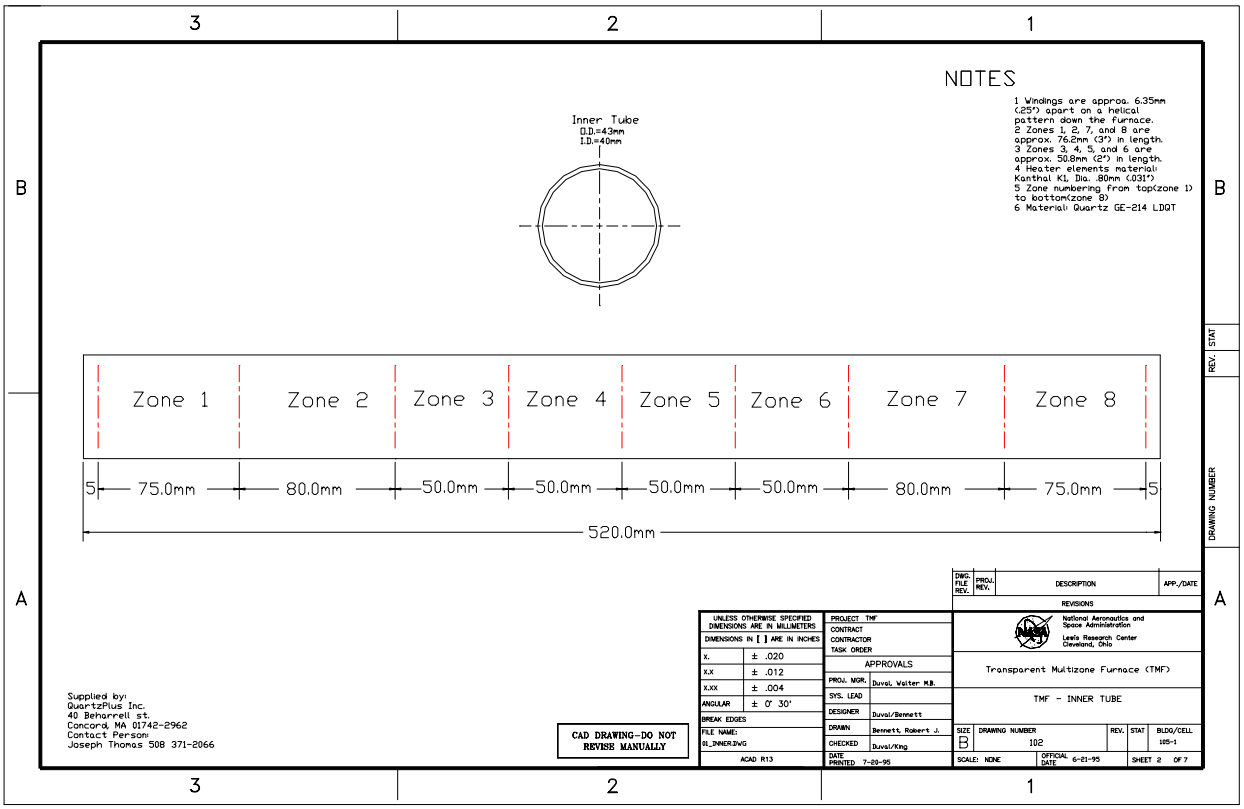
NOTES
1 Windings are approx. 6.35mm (.25") apart on a helical pattern down the furnace.
2 Zones 1, 2, 7, and 8 are approx. 76.2mm (3") in length.
3 Zones 3, 4, 5, and 6 are approx. 50.8mm (2") in length.
4 Heater elements material: Kanthal K1, Dia. .80mm (.031")
5 Zone numbering from top(zone 1) to bottom(zone 8)
6 Material: Quartz GE-214 LDQT
Inner Tube
O.D.=43mm
I.D.=40mm
Zone 1
Zone 2
Zone 3
Zone 4
Zone 5
Zone 6
Zone 7
Zone 8
5
75.0mm
80.0mm
50.0mm
50.0mm
50.0mm
50.0mm
80.0mm
75.0mm
5
520.0mm
Supplied by:
QuartzPlus Inc.
40 Beharrell st.
Concord, MA 01742-2962
Contact Person:
Joseph Thomas 508 371-2066
CAD DRAWING-DO NOT REVISE MANUALLY
UNLESS OTHERWISE SPECIFIED DIMENSIONS ARE IN MILLIMETERS
DIMENSIONS IN [ ] ARE IN INCHES
X. ± .020
X.X ± .012
X.XX ± .004
ANGULAR ± 0° 30'
BREAK EDGES
FILE NAME: 01_INNER.DWG
ACAD R13
PROJECT TMF
CONTRACT
CONTRACTOR
TASK ORDER
APPROVALS
PROJ. MGR. Duval, Walter M.B.
SYS. LEAD
DESIGNER Duval/Bennett
DRAWN Bennett, Robert J.
CHECKED Duval/King
DATE PRINTED 7-20-95
DWG. FILE REV.
PROJ. REV.
DESCRIPTION
APP./DATE
REVISIONS
National Aeronautics and Space Administration
Lewis Research Center
Cleveland, Ohio
Transparent Multizone Furnace (TMF)
TMF - INNER TUBE
SIZE B
DRAWING NUMBER 102
REV.
STAT
BLDG/CELL 105-1
SCALE: NONE
OFFICIAL DATE 6-21-95
SHEET 2 OF 7
DRAWING NUMBER
REV. STAT

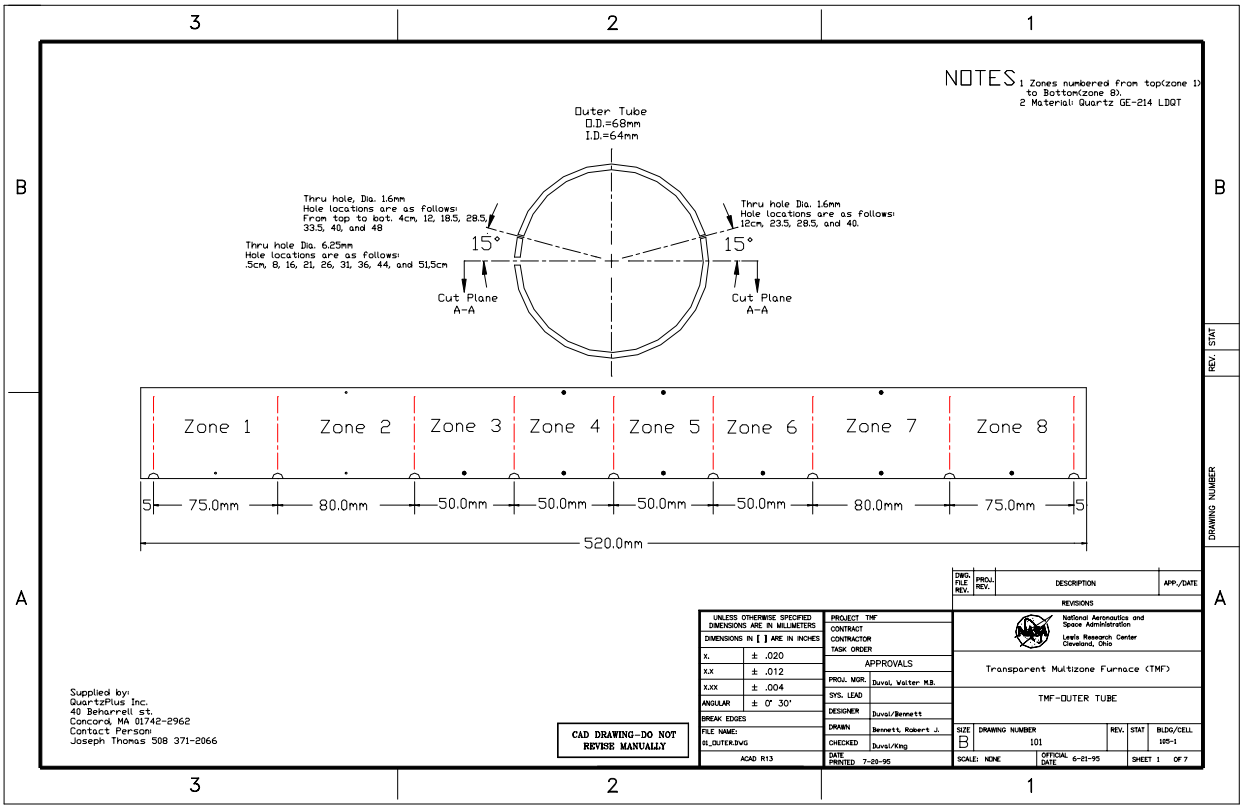
NOTES
1 Zones numbered from top(zone 1) to Bottom(zone 8).
2 Material: Quartz GE-214 LDQT
Outer Tube
O.D.=68mm
I.D.=64mm
Thru hole, Dia. 1.6mm
Hole locations are as follows:
From top to bot. 4cm, 12, 18.5, 28.5, 33.5, 40, and 48
Thru hole Dia. 6.25mm
Hole locations are as follows:
.5cm, 8, 16, 21, 26, 31, 36, 44, and 51.5cm
Thru hole Dia. 1.6mm
Hole locations are as follows:
12cm, 23.5, 28.5, and 40.
15°
15°
Cut Plane A-A
Cut Plane A-A
Zone 1
Zone 2
Zone 3
Zone 4
Zone 5
Zone 6
Zone 7
Zone 8
5
75.0mm
80.0mm
50.0mm
50.0mm
50.0mm
50.0mm
80.0mm
75.0mm
5
520.0mm
Supplied by:
QuartzPlus Inc.
40 Beharrell st.
Concord, MA 01742-2962
Contact Person:
Joseph Thomas 508 371-2066
CAD DRAWING-DO NOT REVISE MANUALLY
UNLESS OTHERWISE SPECIFIED DIMENSIONS ARE IN MILLIMETERS
DIMENSIONS IN [ ] ARE IN INCHES
X. ± .020
X.X ± .012
X.XX ± .004
ANGULAR ± 0° 30'
BREAK EDGES
FILE NAME: 01_OUTER.DWG
ACAD R13
PROJECT TMF
CONTRACT
CONTRACTOR
TASK ORDER
APPROVALS
PROJ. MGR. Duval, Walter M.B.
SYS. LEAD
DESIGNER Duval/Bennett
DRAWN Bennett, Robert J.
CHECKED Duval/King
DATE PRINTED 7-20-95
DWG. FILE REV.
PROJ. REV.
DESCRIPTION
APP./DATE
REVISIONS
National Aeronautics and Space Administration
Lewis Research Center
Cleveland, Ohio
Transparent Multizone Furnace (TMF)
TMF-OUTER TUBE
SIZE B
DRAWING NUMBER 101
REV.
STAT
BLDG/CELL 105-1
SCALE: NONE
OFFICIAL DATE 6-21-95
SHEET 1 OF 7
DRAWING NUMBER
REV. STAT

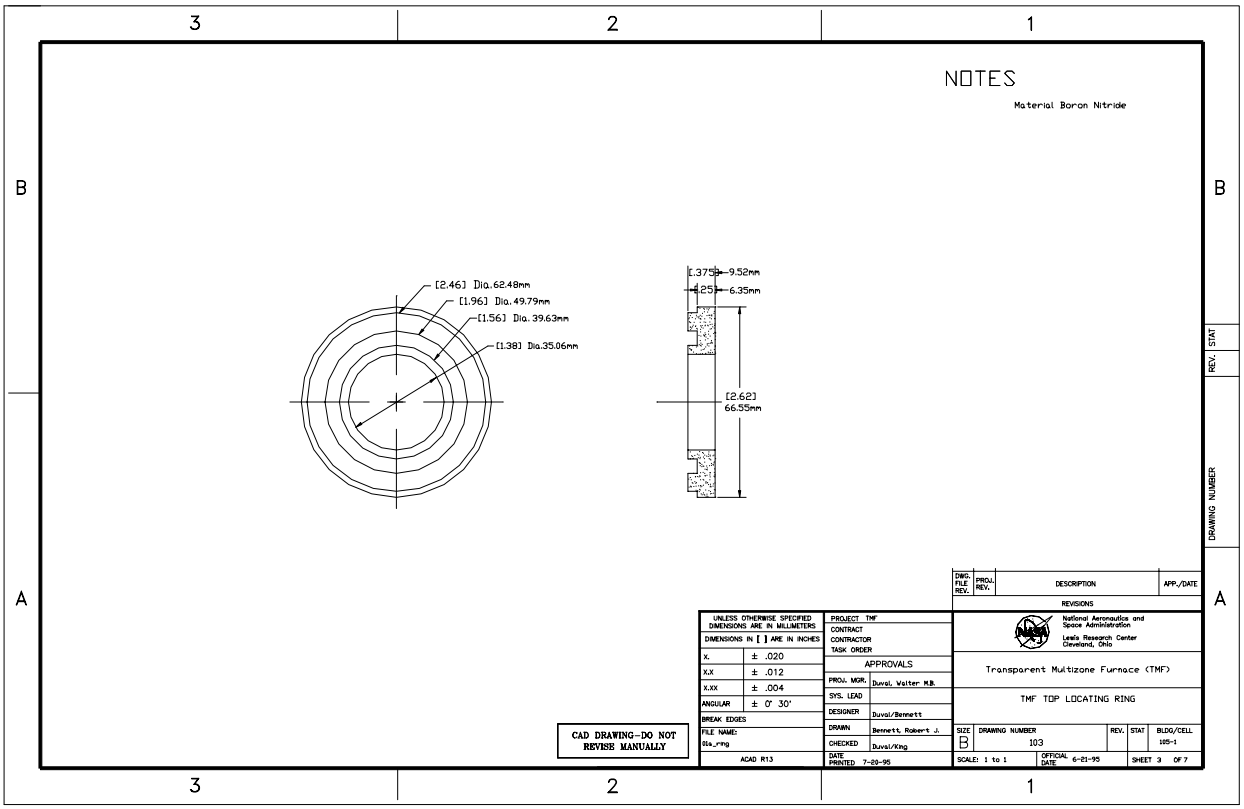
NOTES
Material Boron Nitride
[2.46] Dia.62.48mm
[1.96] Dia.49.79mm
[1.56] Dia. 39.63mm
[1.38] Dia.35.06mm
[.375] 9.52mm
.25 6.35mm
[2.62] 66.55mm
CAD DRAWING-DO NOT REVISE MANUALLY
Transparent Multizone Furnace (TMF)
TMF TDP LOCATING RING
DRAWING NUMBER 103

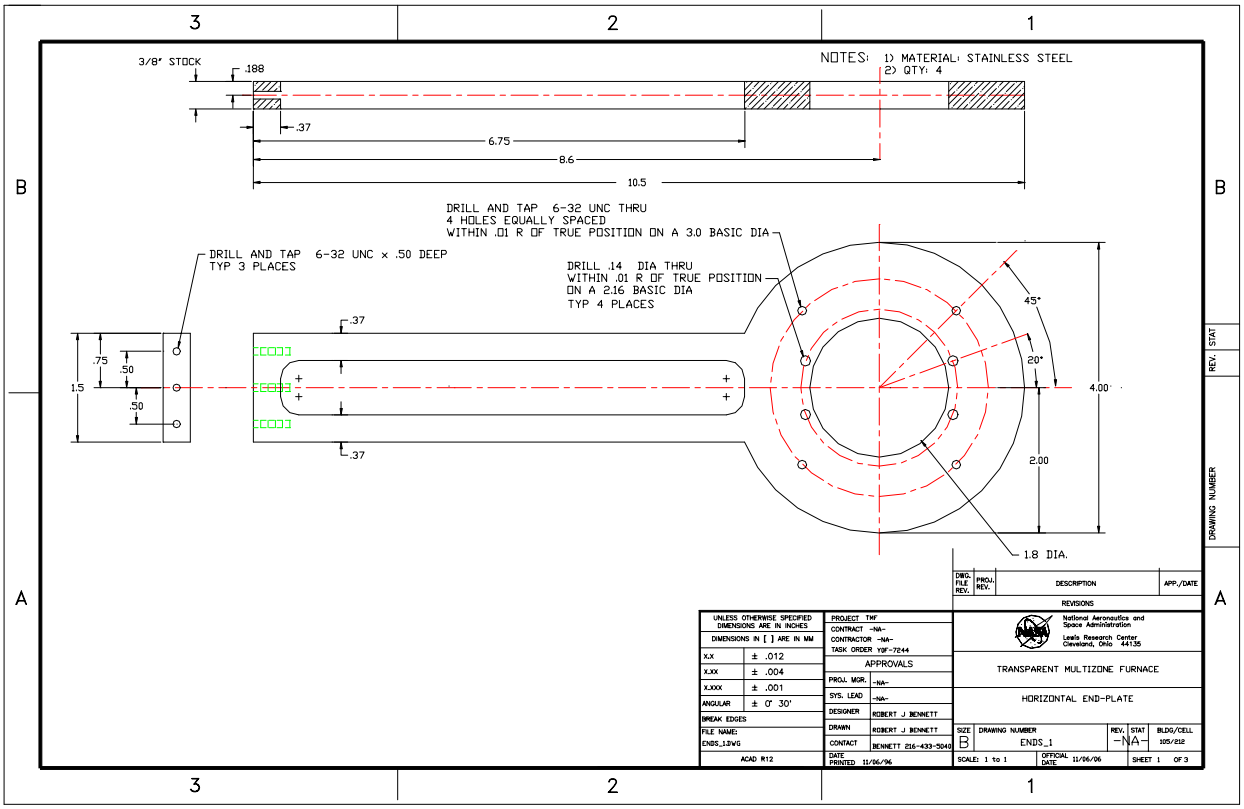
NOTES: 1) MATERIAL: STAINLESS STEEL
2) QTY: 4
3/8" STOCK
.188
.37
6.75
8.6
10.5
DRILL AND TAP 6-32 UNC THRU
4 HOLES EQUALLY SPACED
WITHIN .01 R OF TRUE POSITION ON A 3.0 BASIC DIA
DRILL AND TAP 6-32 UNC x .50 DEEP
TYP 3 PLACES
DRILL .14 DIA THRU
WITHIN .01 R OF TRUE POSITION
ON A 2.16 BASIC DIA
TYP 4 PLACES
.75
.50
1.5
.50
.37
.37
45°
20°
4.00
2.00
1.8 DIA.
TRANSPARENT MULTIZONE FURNACE
HORIZONTAL END-PLATE
DRAWING NUMBER ENDS_1

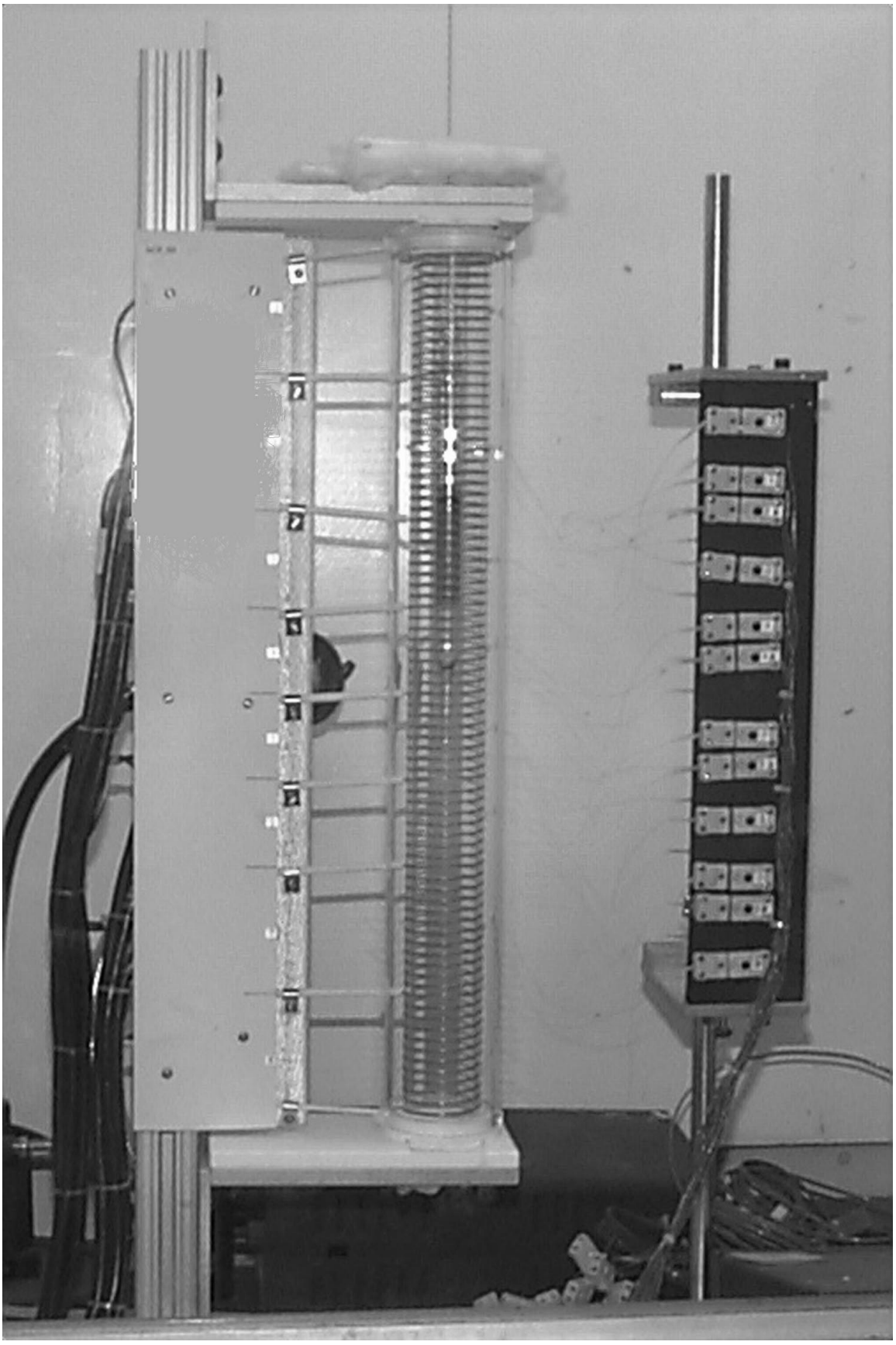

REPORT DOCUMENTATION PAGE

Form Approved
OMB No. 0704-0188

1. AGENCY USE ONLY (*Leave blank*)	2. REPORT DATE	3. REPORT TYPE AND DATES COVERED
	May 1998	Technical Memorandum

4. TITLE AND SUBTITLE

The Design of a Transparent Vertical Multizone Furnace: Application to Thermal Field Tuning and Crystal Growth

5. FUNDING NUMBERS

WU–962–24–00–00

6. AUTHOR(S)

Walter M.B. Duval, Celal Batur, and Robert J. Bennett

7. PERFORMING ORGANIZATION NAME(S) AND ADDRESS(ES)

National Aeronautics and Space Administration
Lewis Research Center
Cleveland, Ohio 44135–3191

8. PERFORMING ORGANIZATION REPORT NUMBER

E–11163

9. SPONSORING/MONITORING AGENCY NAME(S) AND ADDRESS(ES)

National Aeronautics and Space Administration
Washington, DC 20546–0001

10. SPONSORING/MONITORING AGENCY REPORT NUMBER

NASA TM—1998-207412

11. SUPPLEMENTARY NOTES

Prepared for Technology 2007 sponsored by the NASA Tech Briefs, NASA, The Federal Laboratory Consortium, and the Technology Utilization Foundation, Boston, Massachusetts, September 22–24, 1997. Walter M.B. Duval, NASA Lewis Research Center; Celal Batur and Robert J. Bennett, University of Akron, Akron, Ohio 44325–3903. Responsible person, Walter M.B. Duval, organization code 6712, (216) 433–5023.

12a. DISTRIBUTION/AVAILABILITY STATEMENT

Unclassified - Unlimited
Subject Categories: 29, 34, and 31 Distribution: Nonstandard

This publication is available from the NASA Center for AeroSpace Information, (301) 621–0390.

12b. DISTRIBUTION CODE

13. ABSTRACT ***(Maximum 200 words)***

We present an innovative design of a vertical transparent multizone furnace which can operate in the temperature range of 25 ºC to 750 ºC and deliver thermal gradients of 2 ºC/cm to 45 ºC/cm for the commercial applications to crystal growth. The operation of the eight zone furnace is based on a self-tuning temperature control system with a DC power supply for optimal thermal stability. We show that the desired thermal profile over the entire length of the furnace consists of a functional combination of the fundamental thermal profiles for each individual zone obtained by setting the set-point temperature for that zone. The self-tuning system accounts for the zone to zone thermal interactions. The control system operates such that the thermal profile is maintained under thermal load, thus boundary conditions on crystal growth ampoules can be predetermined prior to crystal growth. Temperature profiles for the growth of crystals via directional solidification, vapor transport techniques, and multiple gradient applications are shown to be easily implemented. The unique feature of its transparency and ease of programming thermal profiles make the furnace useful in scientific and commercial applications for determining the optimized process parameters for crystal growth.

14. SUBJECT TERMS

Multizone furnace; Transparent; Crystal growth; Self-tuning controls; Multivariable thermal model

15. NUMBER OF PAGES

25

16. PRICE CODE

A03

17. SECURITY CLASSIFICATION OF REPORT	18. SECURITY CLASSIFICATION OF THIS PAGE	19. SECURITY CLASSIFICATION OF ABSTRACT	20. LIMITATION OF ABSTRACT
Unclassified	Unclassified	Unclassified	